SHOT PEENING CONDITIONS AND PROCESSING PROPERTIES FOR SPRING STEEL

I. Sumiyoshi, A. Tange, H. Okada
NHK SPRING Co.,Ltd., 3-10 Fukuura Kanazawa-ku Yokohama 236-0004, Japan

ABSTRACT
In recent years weight reduction of suspension springs has been increasingly required from the viewpoints of improvement in fuel efficiency of automobiles and global environmental concerns. To realize further weight saving of the suspension spring, it is important to increase its fatigue strength and it is imperative to understand shot peening techniques, which affect improvement in the fatigue strength. However, the relation between surface roughness, residual stress distribution, which affects the fatigue strength, and shot peening conditions has yet to be sufficiently clarified while it is qualitatively comprehended. Moreover, the quantitative relation between surface roughness, residual stress distribution, and fatigue strength has also not been fully understood.
If the fatigue strength can be predicted quantitatively from shot peening conditions, shot peening can be used as a tool for the optimal design of suspension springs. This quantitative prediction will also be very useful in knowing processing conditions to improve the fatigue strength.
In this study, various shot peening conditions, such as shot size and spring steel hardness, were examined to obtain regression formulae to estimate residual stress and surface roughness. Further, a method to predict the fatigue limit from the regression formulae and the fracture mechanics was examined, and its practicality was verified.

KEY WORDS
Shot peening, Spring steel, Shot size, Hardness, Residual stress, Surface roughness, Fracture mechanics

INTRODUCTION
There are few references that enable an estimation of fatigue strength from the hardness of the spring and processing conditions of shot peening though the shot peening process is indispensable for improving the fatigue strength of the spring.
We can choose appropriate processing conditions of shot peening for the purpose of improving the fatigue strength if there is a method to estimate the fatigue strength of the spring from processing conditions of the shot peening. Therefore, such a method would be useful in terms of both cost and quality.
Therefore, we did some experiments on spring steels with different hardness values, using different-sized shots. And we checked the fatigue strength of the specimen under each condition.
From the results of the experimental data, we made regression formulae to lead the residual stress distribution and the surface roughness. And we found a method of estimating the fatigue strength (= fatigue limit) from the processing conditions.

EXPERIMENTAL CONDITIONS AND PROCEDURES
In these experiments, we used SUP7 steel that is used as a general spring steel material in Japan. The chemical composition (wt.%) of SUP7 steel is shown in Table 1. The shape and dimensions of a specimen are shown in Fig.1. After machining, these were oil-quenched at 925℃ and tempered to 400*HV*, 500*HV*, and 600*HV*.
The shape of the specimen was not smooth because the fatigue fracture was caused from the surface.

The condition of shot peening is shown in Table 2. The shot velocity was about 83 m/s. The wheel diameter was ϕ 350 mm. The distance between the specimen surface and the center of the wheel was 530 mm. The rotating velocity of the specimen was 60 rpm.
The type of shot was conditioned cut wire (ccw), and the ccw hardness was 650*HV*.
We used a machine called the Ono type rotating bending fatigue testing machine for the fatigue tests. The fatigue limit of each condition was assumed to be the maximum stress amplitude obtained when the part was not broken at 3.0 x 10^6 cycles.
We investigated the residual stress distribution and the maximum surface roughness of the specimen under each condition.
The specimen was X-rayed to examine the residual stress distribution. The measurement conditions of the residual stress distribution are shown in Table3.

Table 1 Chemical composition of SUP7 (wt.%)

C	Si	Mn	P	S	Cr
0.59	1.92	0.81	0.022	0.012	0.16

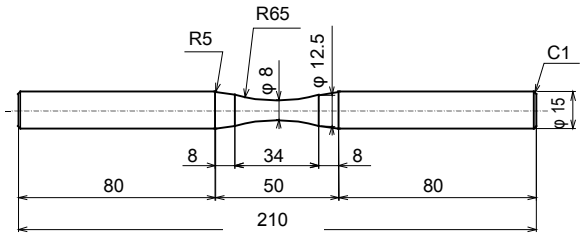

Fig.1 Shape and dimensions of specimen.

Table 2 Shot peening condition.

Shot size *d*	Coverage	Arc height	Fatigue test		
			400 *HV*	500 *HV*	600 *HV*
ö1.5 mm	98-100%	0.79 mm (A)	—	—	—
ö1.2 mm	98-100%	0.66 mm (A)	—	—	—
ö1.0 mm	98-100%	0.54 mm (A)	○	○	○
ö0.8 mm	98-100%	0.50 mm (A)	○	○	○
ö0.6 mm	98-100%	0.35 mm (A)	○	○	○
ö0.4 mm	98-100%	0.20 mm (A)	○	○	○

Table 3 Residual stress measurement conditions.

Characteristics X-ray	Cr-Ká
Diffraction	áFe(211)
2è peak angle [deg]	156.4
Voltage [kV], Current [mA]	30, 10
Area [mm × mm]	1 mm×1 mm
Analysis method	2è-$\sin^2$ø

RESULTS OF EXPERIMENTS

The fatigue limit of each condition decided from the result of fatigue testing is shown Fig. 2.
The fatigue fracture was originated from the surface of the specimen that was broken.
As for the other measurement results the surface compressive residual stress is shown in Fig. 3, the maximum compressive residual stress in Fig. 4, the depth of the maximum compressive residual stress point in Fig. 5, the depth of the zero compressive residual stress point (crossing point) in Fig. 6, and the maximum surface roughness in Fig. 7.

As the specimen got harder and the shot size smaller, the fatigue limit became higher. A clear relationship was not found between the surface compressive residual stress, the specimen hardness, and the shot size.

When the specimen was harder, the maximum compressive residual stress was higher, but the influence of shot size was not significant. When the specimen was harder, and the shot size was smaller, the depth of the maximum compressive residual stress point and the depth of the crossing point were shallower. When the specimen was harder, and shot size was smaller, the maximum surface roughness was smaller.

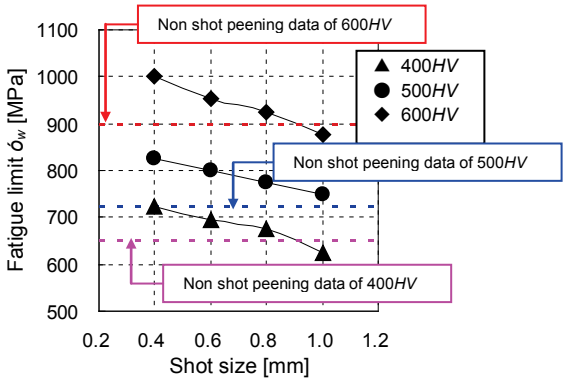

Fig. 2 Relationship between shot size and fatigue limit.

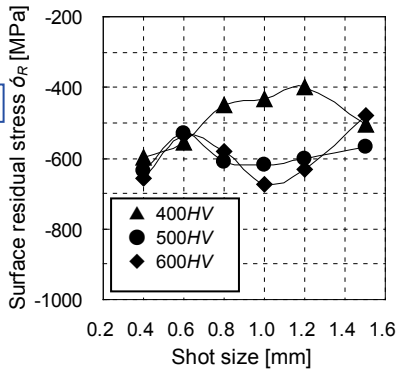

Fig. 3 Relationship between shot size and surface residual stress.

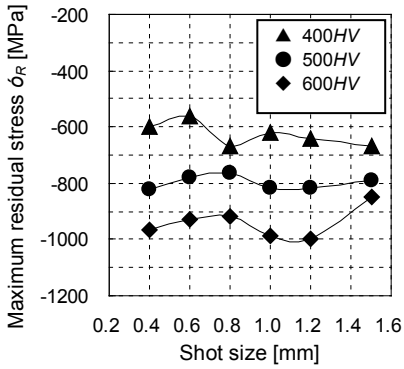

Fig. 4 Relationship between shot size and maximum residual stress.

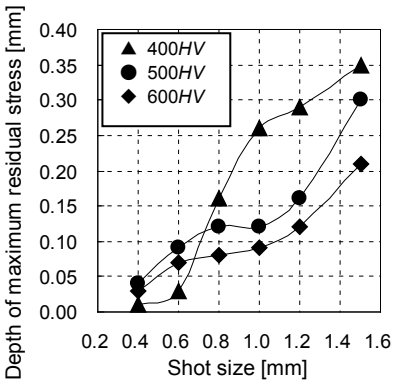

Fig. 5 Relationship between shot size and depth of maximum residual

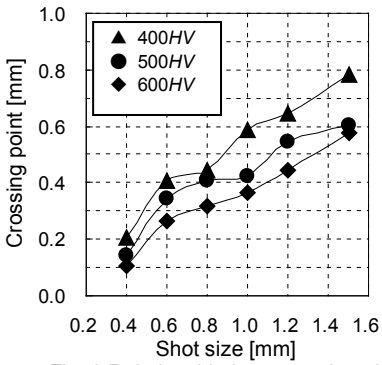

Fig. 6 Relationship between shot size and crossing point.

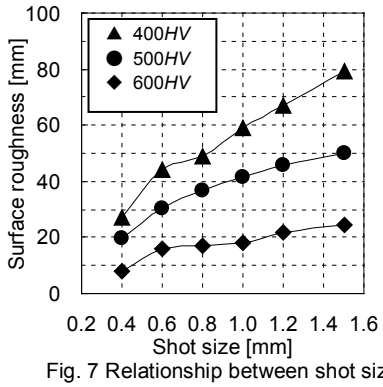

Fig. 7 Relationship between shot size and surface roughness.

DISCUSSION

To predict residual stress and surface roughness from the results of Fig. 2 - Fig. 7, we did a multiple regression analysis to lead the surface residual stress, the maximum residual stress, the depth of the maximum residual stress point, the depth of crossing point, and the maximum surface roughness considering the shot size *d* (m) and the hardness of the specimen *HV* as parameters. The obtained regression formulae are shown in (1) – (5). If the residual stress is compressive, the predicted value is calculated as a minus value. We calculated the predicted values of the surface residual stress, the maximum residual stress, the depth of the maximum residual stress point, the depth of crossing point, and the maximum surface roughness of each condition, and we compared the predicted values and the experimental values.

The results of the comparisons are shown in Fig. 8 − Fig. 10. They indicate good similarity between the predicted values and the experimental values. We can estimate the surface residual stress, the maximum residual stress, the depth of the maximum residual stress point, the depth of the crossing point, and the maximum surface roughness from the shot size and the specimen hardness.

Surface residual stress (MPa)= $7.04\times10^{4}\times d-5.14\times10^{-1}\times HV-3.66\times10^{2}$ ・・・(1)
Maximum residual stress (MPa)= $-6.47\times10^{3}\times d-1.58\times HV+7.80$ ・・・(2)
Depth of maximum residual stress point (m) $=2.30\times10^{-1}\times d-4.17\times10^{-7}\times HV+1.38\times10^{-4}$ ・・・(3)
Crossing point (m) $=4.25\times10^{-1}\times d-8.33\times10^{-7}\times HV+4.49\times10^{-4}$ ・・(4)
Maximum surface roughness (m) $=2.84\times10^{-2}d-1.84\times10^{-7}\times HV+1.02\times10^{-4}$ ・・(5)

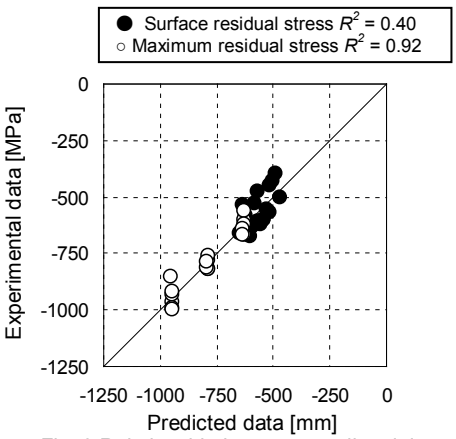

Fig. 8 Relationship between predicted data and experimental data for residual stress.

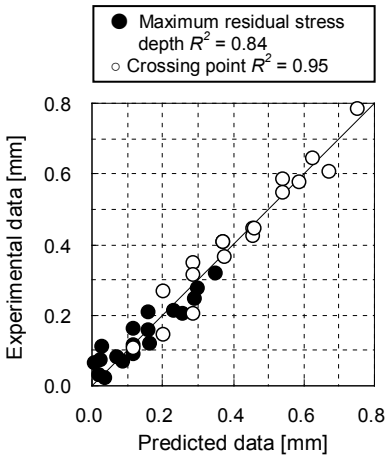

Fig. 9 Relationship between predicted data and experimental data for residual stress

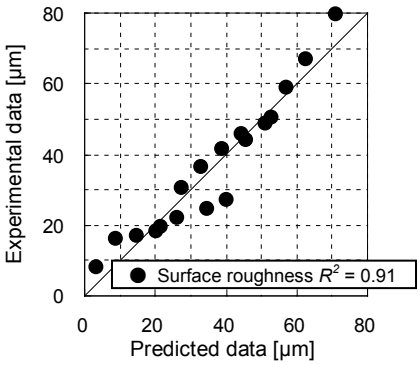

Fig. 10 Relationship between predicted data and experimental data for surface roughness.

Next, we estimated the fatigue limit from the residual stress and the surface roughness predicted by the regression. In this study, we considered the maximum surface roughness to be a small defect, and we evaluated the fatigue limit of the steel that contained the small defect. We used the formulae (6) - (12) to estimate the fatigue limit. The influence of hardness, the small defects, and the stress ratio are all considered in the formulae 6 - 12[(1)(2)].

Fatigue limit containing small crack is given by

$$\Delta\sigma(S)_{th}=\frac{\Delta K(L)_{th}}{\alpha\sqrt{\pi(a+a_0)}} \qquad (6)$$

$$a_0=\frac{1}{\pi}\cdot\left(\frac{\Delta K(L)_{th}}{\alpha\cdot\Delta\sigma_w}\right)^2 \qquad (7)$$

where $\sigma(S)_{th}$ is fatigue limit, and K is stress intensity factor and “a” is crack length.

Range of threshold stress intensity factor containing small crack is given by

$$\Delta K(S)_{th,R=R} = \alpha \cdot \Delta\sigma(S)_{th} \cdot \sqrt{\pi a} = \frac{\Delta K(L)_{th} \cdot \sqrt{a}}{\left[a + \frac{1}{\pi}\left(\frac{\Delta K(L)_{th}}{\alpha \cdot \Delta\sigma_w} \right)^2 \right]^{\frac{1}{2}}} \quad (8)$$

Stress ratio dependency of smooth specimen fatigue limit is given by

$$\frac{\Delta\sigma_{w,R=R}}{2} = \frac{(1-R)}{(1.205 - 0.795 \cdot R)} \cdot \frac{\Delta\sigma_{w,R=-1}}{2} \quad (9)$$

where *R* is stress ratio.

Stress ratio dependency of threshold stress intensity factor containing crack is given by

$$\Delta K(L)_{th,R=R} = (1-R)^{0.75} \cdot \Delta K(L)_{th,R=0} \quad (10)$$

Hardness dependency of smooth specimen fatigue limit under the reverse stress is given by

$$\frac{\Delta\sigma_{w,R=-1}}{2} = 1.6 \cdot HV \quad (11)$$

where HV is hardness of Vickers scale.

Hardness dependency of *threshold stress intensity factor containing crack* under the ulsating stress is given by

$$\Delta K(L)_{th,R=0} = \left(5.514 \cdot 10^{-5} \cdot HV^2 - 0.0775 \cdot HV + 30.335\right) \quad (12)$$

The fatigue limit is calculated from the material hardness, stress ratio (considering residual stress), and defect size that is the maximum surface roughness in this study. In this calculation, we used the residual stress value of the depth that corresponds to the surface roughness. Therefore, we approximated the residual stress distribution to a cubic equation from the surface residual stress value, the maximum residual stress value, and the crossing point. Moreover, there is a report that residual stress decreases when the fatigue testing under the reversed stress is done to the shot peened specimen [(3)]. Then, we compared differences in residual stress between the specimen before testing and the specimen which was not broken at 3 x 10^6 cycles. The compared results are shown in Fig. 11. The residual stress value of the specimen of each hardness decreases by about 90% from the surface to 0.1 mm depth. Therefore, we used 90% residual stress value that corresponded to the depth of the surface roughness when we calculated the fatigue limit.

The result of comparison between the predicted fatigue limit and the experimental fatigue limit is shown Fig. 12. The calculated (predicted) data well corresponded to the experimental data, and we confirmed this method was effective.

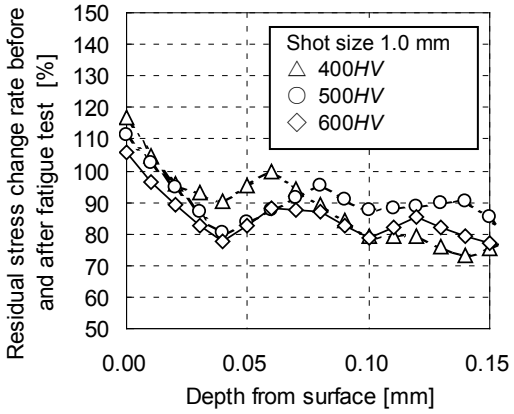

Fig. 11 Residual stress distribution change rate after fatigue test.

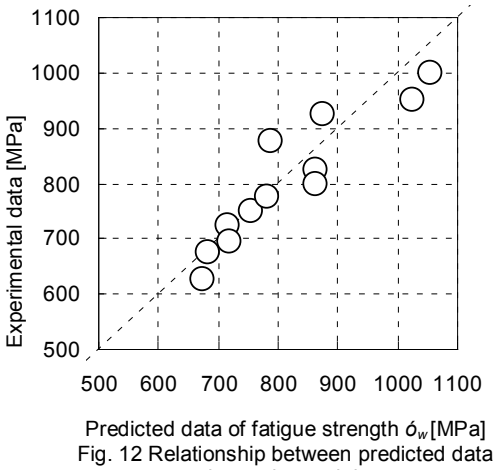

Fig. 12 Relationship between predicted data and experimental data.

CONCLUSIONS

We did some experiments in which we changed the hardness of the spring steel and the shot size of the shot peening, and we checked fatigue strength of some conditions.

(1) From the results of the experimental data, we made the regression formulae to lead the residual stress distribution and the surface roughness.
(2) The calculated (predicted) data well corresponded to the experimental data.
(3) Fatigue limit can be lead easily from an arbitrary shot peening condition.

REFERENCES

（1） A. Tange, T. Akutsu, N. Takamura, Spring essays, No.36,（1991）, 47-53

（2） M. H. El Haddad, T. H. Topper and K. N. Smith Engng Fracture Mech., 11, （1979）, 573-584

（3） S. Otani, R. Kojima, Y. Hagiwara, material, Vol.49, No.7, （2000）, 754-759